

Studies on Systematic Effects of the Trigger on Flavour Tagging at the Generator Level

Internal Note

Issue:	1
Revision:	0
Reference:	2006-046 LHCb Trigger
Created:	August 15, 2006
Last modified:	August 17, 2006
Prepared by:	B. Souza de Paula

Abstract

In this note is presented the systematic effect in the flavour tagging due to the trigger selection. We present a possible way to correct for the different wrong tagging rates for control and signal channels needed for the evaluation of some of the CP asymmetries that will be measured in the experiment. This study is performed at the generator level and uses as decays, $B_s \rightarrow D_s^-(K^+K^-\pi^-)\pi^+$ as the control channel and $B_s \rightarrow J/\psi(\mu^+\mu^-)\phi(K^+K^-)$ and $B_s \rightarrow K^+K^-$ as the signal channels.

1 Introduction

The LHCb experiment has as its main objective to make CP violation precise measurements. For this it is mandatory to know if a B-decay originates as a B or its CP conjugate. Hence one of the indispensable ingredients to measure CP violation in LHCb is the flavour tagging. It is also important to have a precise estimation of the wrong tagging fraction (ω) to know the probability of having a wrong answer from the tagging, where ω is defined as the ratio between the number of wrongly tagged events and the overall number of tagged events. It turns out that it's not possible to measure this ratio directly on some of the CP violating channels because they are not flavour specific. These channels will be treated as *signal channels*. The estimation of ω has to be done by measuring and studying the same fraction in flavour specific decays, or so-called *control channels*.

A comparison of the tagging performance of the different control and signal channels from the Reoptimization TDR [1] shows some striking differences. For instance using $B_s \rightarrow D_s^-(K^+K^-\pi^-)\pi^+$ as control channel for extracting the wrong tagging fraction of the $B_s \rightarrow J/\psi(\mu^+\mu^-)\phi(K^+K^-)$ or the $B_s \rightarrow K^+K^-$ considering the ratios as being the same would imply a serious bias since the ω obtained from MC truth data of the channels are not in agreement, as is shown in table 1.

$B_s \rightarrow D_s^-\pi^+$	$B_s \rightarrow J/\psi\phi$	$B_s \rightarrow K^+K^-$
30.0 ± 1.6	33.4 ± 0.4	33.0 ± 0.8

Table 1 ω values obtained from MC truth on the Reoptimization TDR for the studied control and signal channels.

In this study, in order to get the ω values for the *signal channels*, unlike what will happen when the experimental data comes, we have access and use the MC truth information to know if the B-signal originated as a B_s or a \bar{B}_s .

In principle the tagging efficiency and correctness probability should be the same for a given B meson independently of its decay products, providing there is no selection which affects the phase space of the signal B-meson differently for different decays. But for two distinct decays, for instance a signal and a control channels, the decay products of the B will be unequally distributed in phase space. In applying the trigger selection on these two channels the phase space of the B meson can be differently affected. Hence, by changing the phase space of the signal B and due to the correlations between this meson and other particles on the event, especially the other b quark from the pair that originated the signal B, there is no reason to expect tagging performances of a control and a signal channels to be the same after trigger selection. And we can

expect this systematic effect to generate an even bigger difference after applying the offline selections, which have different cuts for each channel. The overall differences in the simulation of LHCb can be verified in comparing the performance for different channels in the Reoptimization TDR [1, 2].

The difference in the tagging efficiency, ϵ_{tag} , which is the probability for a selected event to have a tagging decision, can be directly measured in each channel individually and can even be used as a hint that the bias in the samples are different.

It is then very important to verify the existence of and try to correct for the differences in ω , in order to be able to extract a correct value for the signal channel from the measurement of ω in the control channel. The goal of the present note is to show the studies that were done in this direction suggesting a possible solution for the problem in correcting for the phase space difference introduced by the trigger selection. For that the decay used as control channel was $B_s \rightarrow D_s^- (K^+ K^- \pi^-) \pi^+$ to compare with two signal channels: $B_s \rightarrow J/\psi (\mu^+ \mu^-) \phi (K^+ K^-)$ and $B_s \rightarrow K^+ K^-$.

It was chosen to start this study at the generator level, using PYTHIA [3]. This in order to be able to handle only the bias introduced by the trigger selection in the tagging due to the kinematic correlations between the particles and verify that the method intended for the correction is valid without too many complications. Only single pp interactions are used but the settings are the same used in the Reoptimization TDR studies. Being so it is not the objective of the present study to obtain accurate individual numbers of ϵ_{tag} and ω that will match the measurements of LHCb but to correct for discrepancies between channels. Other effects that can contribute to this bias in the experiment, such as reconstruction inefficiency or particle identification and especially the offline selection as well, can be studied later in the existing full simulation of the experiment.

2 Trigger and tagging simulation

2.1 Trigger

Working at generator level a mimicking of the trigger decisions was needed. One of the goals of the study being to avoid any unnecessary complication it was tried to mimic the trigger levels L0 and L1 in a very simple way and all the kinematic variables used for the cuts were the MC generated ones except for the impact parameter with respect to the primary vertex, in which a smearing is applied as a function of the particle P_T .

I try to reproduce L0 by searching for the highest P_T muon, electron or positron and hadron within the geometrical acceptance of the experiment, which was taken to be the straight line extrapolation of the tracks to the Trigger Tracker station TTb. The cuts applied to these particles are similar to the ones actually used in the trigger software as attests table 2.

For L1 is calculated the L1 global variable, without any bonus, using the two highest P_T charged particles with $I_P > 200 \mu\text{m}$ with respect to the primary vertex in the spectrometer acceptance [4]. The cut is made such that 40 kHz of minimum bias events are accepted. A smearing of the impact parameter is done to avoid the $I_P = 0$ of the particles coming from the primary vertex since the I_P significance is used in the L1 variable calculation. The resolution used depends on the P_T , is shown in figure 1 and is obtained with the formula [5]:

Particle	Generator level P_T cut (GeV/c)	Full Simulation E_T cut (GeV)
μ	> 1.2	> 1.1
e	> 2.6	> 2.8
hadron	> 3.5	> 3.6

Table 2 Minimum values for P_T and E_T used as trigger in L0 respectively in this generator level and in the full simulation

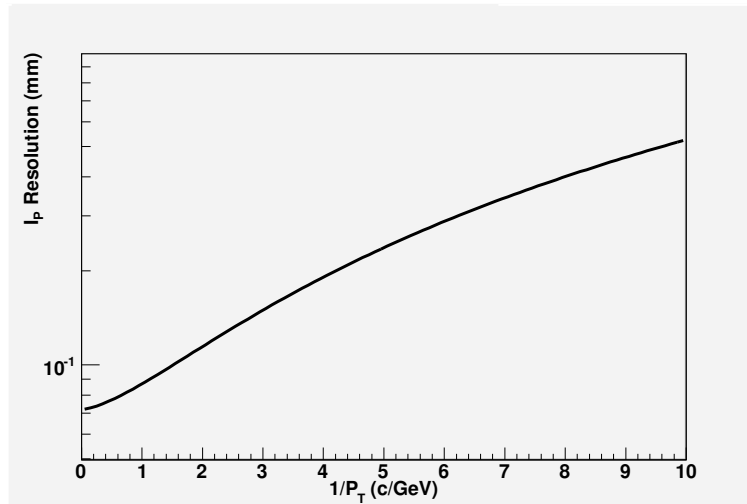


Figure 1 Impact parameter smearing with respect to the primary vertex resolution as a function of P_T applied to the true Monte Carlo value

$$\sigma(I_P)/\text{mm} = 0.072 + (206 \ln(P_T/\text{MeV}) - 1.27) (P_T/\text{MeV})^{-1.66}$$

To take into account the effect of the bias brought by the di-muon trigger on channels with di-muons, which is the case of one of the studied signal channels, any event having two muons in the geometrical acceptance is considered to trigger L1 independently of its variable value.

The trigger efficiencies obtained in this very simple simulation are compared with the ones in the Trigger TDR [4] for the studied channels in table 3. Also in this table are shown the total number of generated events and the geometrical acceptance efficiency, which corresponds to have all the signal products inside the acceptance. The selection is done in steps which means that only events inside the geometrical acceptance can be triggered and only L0 selected events are considered for L1 selection.

It's noticeable that the efficiency of the geometrical acceptance is already different between the channels and may also introduce a difference in the tagging ratios, in a similar way as the offline selection. An important effect is the 100 % L1 efficiency for the

Channel	# Evt	ϵ_{geo}	ϵ_{L0}	TDR ϵ_{L0}	ϵ_{L1}	TDR ϵ_{L1}
$B_s \rightarrow D_s \pi$	17.8 M	12.193 ± 0.008	59.11 ± 0.03	49.4 ± 0.6	65.75 ± 0.04	63.0 ± 0.9
$B_s \rightarrow J/\psi \phi$	12 M	12.271 ± 0.009	99.421 ± 0.006	89.7 ± 0.1	100 ± 0	71.4 ± 0.2
$B_s \rightarrow KK$	14.5 M	14.829 ± 0.009	79.98 ± 0.03	51.8 ± 0.3	60.21 ± 0.04	60.0 ± 0.4

Table 3 Number of generated events, geometrical acceptance and trigger efficiencies for the studied channels compared with Trigger TDR trigger efficiencies [4]. The uncertainties are statistical.

Selection		$B_s \rightarrow D_s \pi$	$B_s \rightarrow J/\psi \phi$	$B_s \rightarrow KK$
Geo	ϵ_{tag}	39.96 ± 0.03	40.27 ± 0.04	39.03 ± 0.03
	ω	26.69 ± 0.05	27.07 ± 0.06	26.77 ± 0.05
L0	ϵ_{tag}	45.14 ± 0.04	40.33 ± 0.04	41.72 ± 0.04
	ω	25.10 ± 0.06	27.05 ± 0.06	26.10 ± 0.05
L1	ϵ_{tag}	47.15 ± 0.05	40.33 ± 0.04	43.72 ± 0.05
	ω	24.63 ± 0.07	27.05 ± 0.06	25.65 ± 0.06
	ϵ_{eff}	12.14 ± 0.03	8.49 ± 0.02	10.37 ± 0.03

Table 4 Tagging efficiency and wrong tagging fraction for the geometrical accepted, L0 and L1 selected events for the signal and control channels. Also the effective tagging efficiency for the L1 selected events is shown.

$B_s \rightarrow J/\psi \phi$ channel because of the di-muon implementation: all the geometrical accepted events will have both muons inside the acceptance and hence will be accepted by the di-muon L1 trigger, if they passed L0. This effect will potentially enhance the difference in the tagging bias between the two different samples as this means that the $B_s \rightarrow J/\psi \phi$ will pass L1 without any kinematic bias. Being so, and having in mind that the purpose is to correct for such bias rather than have very accurate individual numbers for the studied ratios, it is an acceptable and maybe even a wanted effect.

2.2 Tagging

The same kind of mimicking which was done for the trigger was needed to define the tagging particles. The same cuts were used for the tagging as for the full simulation. So for the opposite tags an electron or a muon having $p > 5\text{GeV}/c$, $P_T > 1.2\text{GeV}/c$ or a kaon having $p > 3\text{GeV}/c$, $P_T > 0.4\text{GeV}/c$ and $I_P/\sigma > 3.7$ in the acceptance was considered to be a tagging particle. Where the I_P is again with respect to the true primary vertex. The resolution of the impact parameter used was the one already mentioned in the previous section.

In the same way for the same-side tagging a kaon having $p > 4\text{GeV}/c$, $P_T > 0.4\text{GeV}/c$, $I_P/\sigma < 2.5$ (with respect to the primary vertex and the same resolution as before), $|\Delta\eta| < 1$, $|\Delta\phi| < 1.1$ and $|\Delta m| < 1.5\text{GeV}/c^2$ was considered as a tag (K_{same}). Where the difference in pseudo-rapidity and polar angle is between the kaon and the signal B_s and the mass difference is between the signal B_s and the combination $B_s K$.

The only differences in this tagging algorithm and the one used in the full simulation are the absence of the vertex charge tagging and also if more than one tagging particle is present in an event. In this case the decision was taken according to the majority of tags independently of the type of tagging. If there was an equal number of b and \bar{b} tags the event was considered as untagged.

The results obtained for the tagging efficiency ϵ_{tag} and the wrong tagging fraction ω in the different steps of the selection are shown in tables 4 (for the overall tagging) and 5 (for each type of tagging particle) together with the effective tagging efficiency ϵ_{eff} for events accepted by all selections. Where $\epsilon_{\text{eff}} = \epsilon_{\text{tag}} (1 - 2\omega)^2$.

From these tagging results it is possible to see that even before the trigger selection the channels present slightly different tagging performances, which is introduced by the same-side kaon. This can be understood looking at the different values for ϵ_{geo} in table 3 and remembering that the same-side tagging depends directly on the phase space

		μ			e		
Selection		$B_s \rightarrow D_s\pi$	$B_s \rightarrow J/\psi\phi$	$B_s \rightarrow KK$	$B_s \rightarrow D_s\pi$	$B_s \rightarrow J/\psi\phi$	$B_s \rightarrow KK$
Geo	ϵ_{tag}	4.77 ± 0.01	4.78 ± 0.02	4.77 ± 0.01	4.88 ± 0.01	4.93 ± 0.02	4.89 ± 0.01
	ω	25.6 ± 0.1	25.8 ± 0.2	25.4 ± 0.1	26.2 ± 0.1	26.3 ± 0.2	26.1 ± 0.1
L0	ϵ_{tag}	8.07 ± 0.02	4.81 ± 0.02	5.97 ± 0.02	5.88 ± 0.02	4.94 ± 0.02	5.21 ± 0.02
	ω	25.6 ± 0.1	25.8 ± 0.2	25.4 ± 0.1	25.8 ± 0.2	26.3 ± 0.2	25.8 ± 0.1
L1	ϵ_{tag}	9.43 ± 0.03	4.81 ± 0.02	7.23 ± 0.03	6.74 ± 0.03	4.94 ± 0.02	6.14 ± 0.02
	ω	26.5 ± 0.2	25.8 ± 0.2	26.5 ± 0.2	26.7 ± 0.2	26.3 ± 0.2	26.7 ± 0.2
	ϵ_{eff}	2.08 ± 0.01	1.13 ± 0.01	1.60 ± 0.01	1.46 ± 0.01	1.10 ± 0.01	1.33 ± 0.01
		K_{opp}			K_{same}		
Selection		$B_s \rightarrow D_s\pi$	$B_s \rightarrow J/\psi\phi$	$B_s \rightarrow KK$	$B_s \rightarrow D_s\pi$	$B_s \rightarrow J/\psi\phi$	$B_s \rightarrow KK$
Geo	ϵ_{tag}	10.19 ± 0.02	10.26 ± 0.02	10.24 ± 0.02	29.09 ± 0.03	29.39 ± 0.04	27.79 ± 0.03
	ω	19.89 ± 0.08	19.8 ± 0.1	19.83 ± 0.08	31.09 ± 0.06	31.63 ± 0.07	31.42 ± 0.06
L0	ϵ_{tag}	10.69 ± 0.03	10.26 ± 0.03	10.30 ± 0.02	32.56 ± 0.04	29.43 ± 0.04	30.15 ± 0.03
	ω	19.5 ± 0.1	19.7 ± 0.1	19.7 ± 0.1	29.28 ± 0.07	31.61 ± 0.07	30.48 ± 0.06
L1	ϵ_{tag}	12.83 ± 0.04	10.26 ± 0.03	12.94 ± 0.03	32.63 ± 0.05	29.43 ± 0.04	29.73 ± 0.04
	ω	19.3 ± 0.1	19.7 ± 0.1	19.6 ± 0.1	29.09 ± 0.09	31.61 ± 0.07	30.58 ± 0.08
	ϵ_{eff}	4.83 ± 0.02	3.78 ± 0.02	4.77 ± 0.02	5.70 ± 0.02	3.98 ± 0.02	4.47 ± 0.02

Table 5 Tagging efficiency and wrong tagging fraction for the geometrical accepted, L0 and L1 selected events for the signal and control channels sorted according to the tagging particle. The effective tagging efficiency is also shown for the L1 selected events.

of the signal B because of the cuts applied to it. But the striking effect can be noticed following the values of ϵ_{tag} and ω throughout the trigger selection and remarking how the differences between the channels get bigger in the same-side and are introduced in the opposite tagging. This of course makes the overall tagging performance completely different between the $B_s \rightarrow D_s\pi$ and the signal channels for the majority of the categories. So it is clear that it would not be correct to measure the wrong tagging fraction in the control sample and apply it blindly to the signal channels.

With a very simple mimicking of the trigger and tagging at the generator level it was then possible to introduce a clear difference in the tagging bias between a signal and a control channel due to the geometrical acceptance and trigger selection. Once more it is worth saying that we are not interested in reproducing the Optimization TDR numbers but in correcting the effect so that the tagging performance of the studied signal channel can be correctly obtained from the control channel.

3 The correlation

As already mentioned the difference in the tagging performance between the channels could be expected and should originate from a difference in the phase space of the B hadrons, both for the signal and the tagging B-hadrons. Figures 2 and 3 show the comparison of the P_T and the proper lifetime τ for both the signal and the tagging B between the control channel and the $B_s \rightarrow J/\psi\phi$ after the trigger selection. One sees that indeed the phase space of the signal B was transformed in a completely different way in the two channels. This effect was foreseen but a less obvious consequence observed is that the selection also created a difference in the tagging B phase space.

Correcting for these phase space differences should be enough to correct also the tagging disagreements. But when the experiment is running we will not always recon-

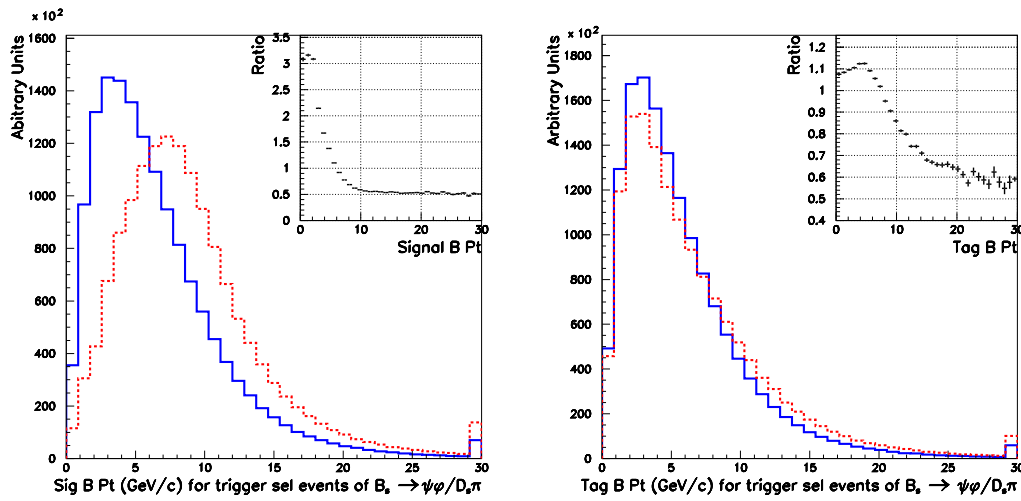


Figure 2 P_T distributions for the signal B in the left and tagging B in the right between the control channel (dashed line) and the $B_s \rightarrow J/\psi\phi$ (solid line) after trigger selection. The distributions are normalized to have the same area and the ratio between the plots is presented in the top right corner of each plot.

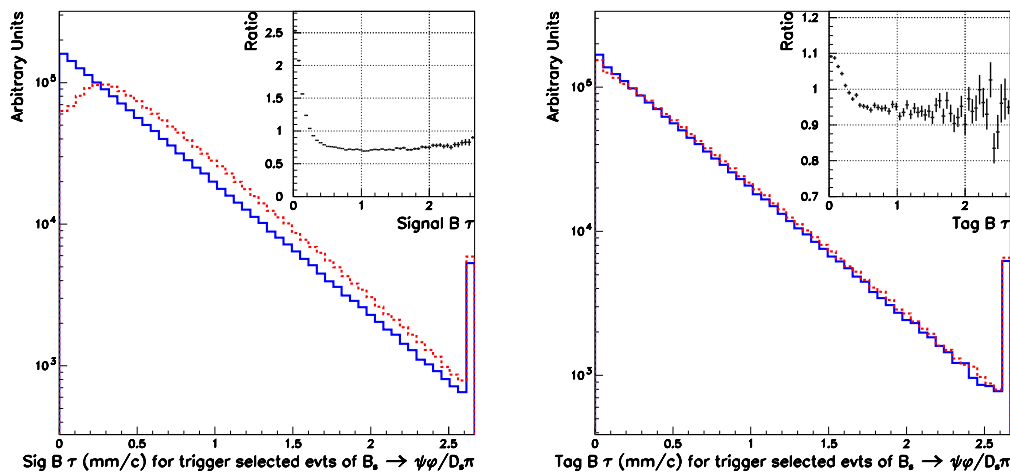


Figure 3 Proper time distributions for the signal B in the left and the tagging B in the right for the control channel (dashed line) and the $B_s \rightarrow J/\psi\phi$ (solid line) after trigger selection. The distributions are normalized to have the same area and the ratio between the plots is shown in the top corner of each plot.

struct the tagging B so we cannot use the tagging B information for the correction. The only informations that will always be available is what concerns the signal and its products. The solution could be that in correcting only for the signal phase space, but taking rightly into account the correlation between the $b\bar{b}$ pair produced, the wrong tagging fraction would be also corrected for.

The main cuts applied by the trigger selection are on P_T so it should be expected that this is the most affected variable after selection. The idea is then try to correct only for these P_T distributions. But as shown in figure 3 we are dealing still with quite different biased samples. Because of the di-muon trigger the $B_s \rightarrow J/\psi\phi$ sample will always trigger in L1, while the control sample might be selected due to a tagging B with a significant lifetime. This means that not knowing the tagging B phase space one is not able to correct ω by looking at the signal B only. So in order to proceed the events were sorted according to the trigger selection in a way that will allow the wanted correction.

3.1 Trigger categories

The obvious difference in the trigger selection between the channels is introduced when the signal products were responsible for the trigger. According to this it was decided to sort each trigger step in to 3 categories:

- Trigger On Signal (TOS) - These are events that were or would be triggered only by applying the cuts on the studied signal B decay products.
- Trigger Independent of Signal (TIS) - These are events that would be triggered even if the signal B and its decay products were not present in the event at all.
- Trigger On Both (TOB) - These are the triggered events that do not fit in the other categories. This means that they need both the signal products and the rest of the event to be selected by the trigger.

The sorting in these categories is shown in a flow diagram as they are sorted in the study in table 6. From the definitions and flow diagrams it is possible to verify that an event can be at the same time both TOS and TIS but the TOB category is exclusive. From this sorting structure we can expect that in the TOS events, where all the kinematic requirements were applied to the signal only, the signal phase space is rather strongly affected, possibly in a very different way for the channels. This will also affect the rest of the event, but the change in the tagging part of the event is introduced only through its correlation with the signal-B. Hence, comparing the tagging performance between signal and control channels in an infinitesimal small volume of signal B phase space should render the same tagging performance.

In a TIS event all the trigger requirements are made independently of the signal products so the phase space of the whole tagging part of the event should be dramatically affected together with the tagging ratios. But since the signal part was ignored in the selection the introduced difference should be the same both for the signal and the control channels. In this sense TIS events are expected to give the same tagging performance for any channel.

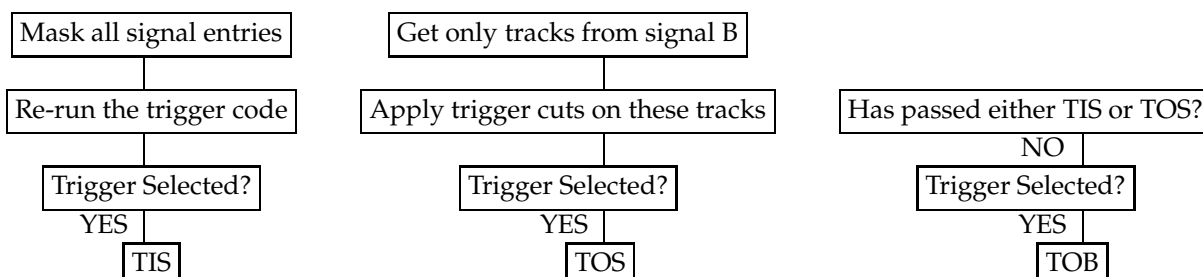


Table 6 Diagram showing how the sorting in trigger categories is done

In that way we sorted the events in two samples. The first in which the tagging depends only on the signal phase space and can then be corrected using the signal part of the event, to which we will have full access in the experiment. The other sample in which the tagging part phase space to which we cannot have full access is heavily affected but in the same way for all the channels.

The remaining events are classified as TOB. The treatment they should receive so that the control channel can reproduce the signal channel is less straightforward. This because here the cuts are applied at the same time both in the signal and the tagging part of the event so that the reasoning used to explain why the correction should not be done directly without the sorting in trigger selection categories applies. For the moment there is still no solution for these events but we will show the results applying the same correction mechanism as for the TIS and TOS events.

This division applies to each trigger level. So in principle there would be 9 different categories: L0 and L1 TOS, L0 TOS and L1 TIS and etc. But our L0 is a one particle trigger so there is no way we have a trigger accepted event that is not TIS or TOS so we have no TOB L0. Also since the di-muon trigger gives 100 % efficiency there will be no L1 TOB for the $B_s \rightarrow J/\psi\phi$.

In order to make the phase space correction we need exclusive categories which is not the case for TIS and TOS. To solve this one should keep in mind that before any selection is done the tagging performance of the channels should be the same. After applying a TIS selection it was already said that the change happens identically for two different decays. In the same way the phase space of the events that were not TIS selected should be equal as well. By applying now a TOS selection in these remaining events the difference that arises in the tagging performance is due to the correlation with the signal alone. That means that the signal phase space correction mentioned before should be enough to obtain the right values. Hence by treating as exclusive categories TIS and "TOS and not TIS" the correction should work. From now on in this note when we say TOS we mean "TOS and not TIS" to deal with the final categories. And this reasoning applies for a sequence of selections so we will work with the following exclusive trigger categories in order of selection:

1. L0 TIS & L1 TIS
2. L0 TIS & L1 TOS
3. L0 TIS & L1 TOB
4. L0 TOS & L1 TIS
5. L0 TOS & L1 TOS

Channel	$\frac{\epsilon_{L0TOS}}{\epsilon_{L0}}$	$\frac{\epsilon_{L0TIS}}{\epsilon_{L0}}$
$B_s \rightarrow D_s^- \pi^+$	64.54 ± 0.06	35.46 ± 0.05
$B_s \rightarrow J/\psi\phi$	78.92 ± 0.05	21.08 ± 0.07
$B_s \rightarrow K^- K^+$	74.18 ± 0.05	25.82 ± 0.04

Table 7 Contribution of the two L0 exclusive categories for events inside the geometrical acceptance for the signal and control channels.

	L0 TOS		
	L1 TOS	L1 TIS	L1 TOB
$B_s \rightarrow D_s \pi$	39.89 ± 0.05	13.04 ± 0.03	8.12 ± 0.03
$B_s \rightarrow \psi\phi$	64.89 ± 0.04	14.03 ± 0.03	0 ± 0
$B_s \rightarrow KK$	32.19 ± 0.04	16.93 ± 0.03	22.39 ± 0.03
	L0 TIS		
	L1 TOS	L1 TIS	L1 TOB
$B_s \rightarrow D_s \pi$	20.19 ± 0.06	14.09 ± 0.05	4.67 ± 0.03
$B_s \rightarrow \psi\phi$	15.09 ± 0.06	5.99 ± 0.04	0 ± 0
$B_s \rightarrow KK$	9.22 ± 0.04	11.41 ± 0.05	7.86 ± 0.04

Table 8 The percentage of events in each of the exclusive trigger categories for the signal and control channels.

6. L0 TOS & L1 TOB

The contribution of each of the exclusive categories is shown in tables 7 for L0 and 8 for L1 selections. From these we can see very different contributions from the categories for each of the channels. An important feature already mentioned is the lack of TOB events for the $B_s \rightarrow J/\psi\phi$ channel.

4 $B_s \rightarrow J/\psi\phi$

4.1 Phase Space Differences

To start with less categories and also because the TOB events are expected to be more difficult to study I start trying to correct the bias in ω between the $B_s \rightarrow J/\psi\phi$ and the control channel.

From the reasoning given to explain why the sorting in trigger categories is needed we should expect different behaviors for them. For instance in the sample that was entirely TIS selected both the signal and the other B of the event should present the same phase space distributions for different channels. Figure 4 shows the P_T distributions for the signal and tagging B for both channels in events that passed the L0 and L1 TIS selection.

From these plots it is possible to see that the differences between channels is small but exists. This happens because in every selection we have the geometrical acceptance requirement which is a TOS selection itself as it is applied only in the signal products. But looking at the efficiencies of this selection in table 4 we can expect the difference brought by this selection to be small, especially for the $B_s \rightarrow J/\psi\phi$. Also as the geometrical acceptance cut is a TOS selection the signal B phase space should be more affected by it than the tagging B. The distributions of the transverse momentum for these events are shown in figure 5, where we can verify, especially in the ratio plots, both that the

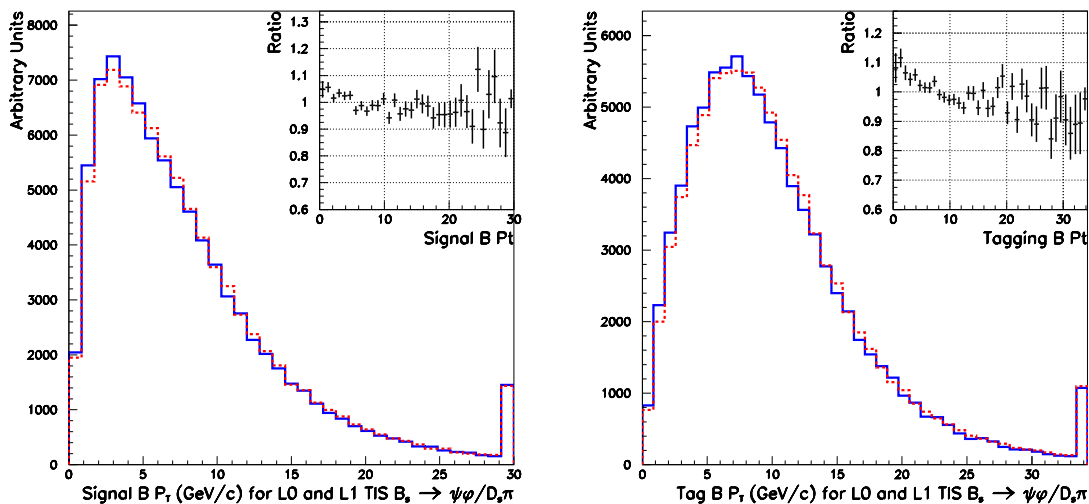


Figure 4 P_T distributions of the signal B in the left and the tagging B in the right for the control channel (dashed line) and the $B_s \rightarrow J/\psi\phi$ (solid line) after a L0 and L1 TIS trigger selection. The distributions are normalized to have the same area and the ratio of the distributions is shown on the top right corner.

differences in the distributions are there even before applying the trigger selection and that the signal B is more affected by it.

On the other hand one should expect a quite bigger difference in the bias of the entirely TOS selected sample. Figure 6 shows the transverse momentum distributions for the L0 and L1 TOS selected events for both channels. From these plots it becomes clear that indeed the TOS selection makes these distributions completely different while this effect is much milder in a TIS one. The plots for the two remaining categories are shown in figures 7 and 8.

A clear conclusion one can arrive at from the distributions is that the L0 selection is the main responsible for creating an unequal bias in the P_T samples. This can be said as in the two categories with a TOS selection in L0 the ratios of the plots are completely different while in the L0 TIS they look much more alike, even for the L1 TOS. Also because of that in the signal B P_T distributions the differences are much more striking than in the tagging B. This is a good indication that the opposite side tagging will be less affected as will be shown later.

Another important variable for the tagging performance is the proper lifetime of the tagging B. If the event was tagged by a particle coming from this meson, a bigger τ will translate into a larger probability of oscillation before the decay. We know that if the tagging B oscillated before the decay it will most likely give a wrong tagging answer. The difference of τ between the channels was already shown in figure 3 for the whole sample of trigger selected events. Just as for the P_T each of the categories will affect τ in a way.

As τ do not depend directly on the kinematic variables, the tagging B τ should not be affected through correlation by any TOS selection. Hence the completely TOS selection should bring no differences in this variable. Meanwhile the cuts in I_P from the trigger should create a difference to the signal B lifetime. Both predictions can be verified in figure 9. Only in L1 there are I_P requirements on the particles hence, following the same

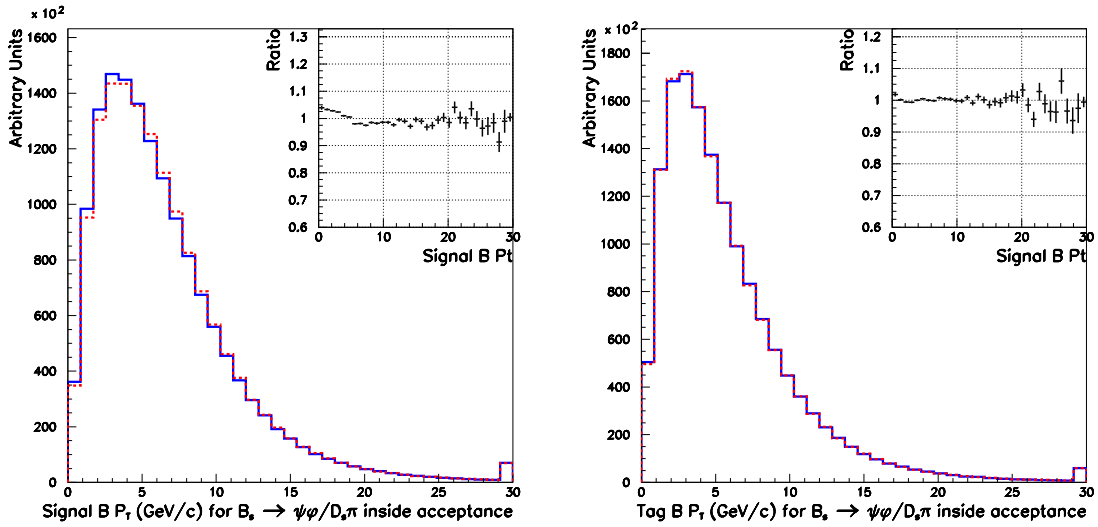


Figure 5 P_T distributions of the signal B in the left and the tagging B in the right for the control channel (dashed line) and the $B_s \rightarrow J/\psi\phi$ (solid line) for events with the signal B products inside the detector acceptance. The distributions are normalized to have the same area and the ratio of the distributions is shown on the top right corner.

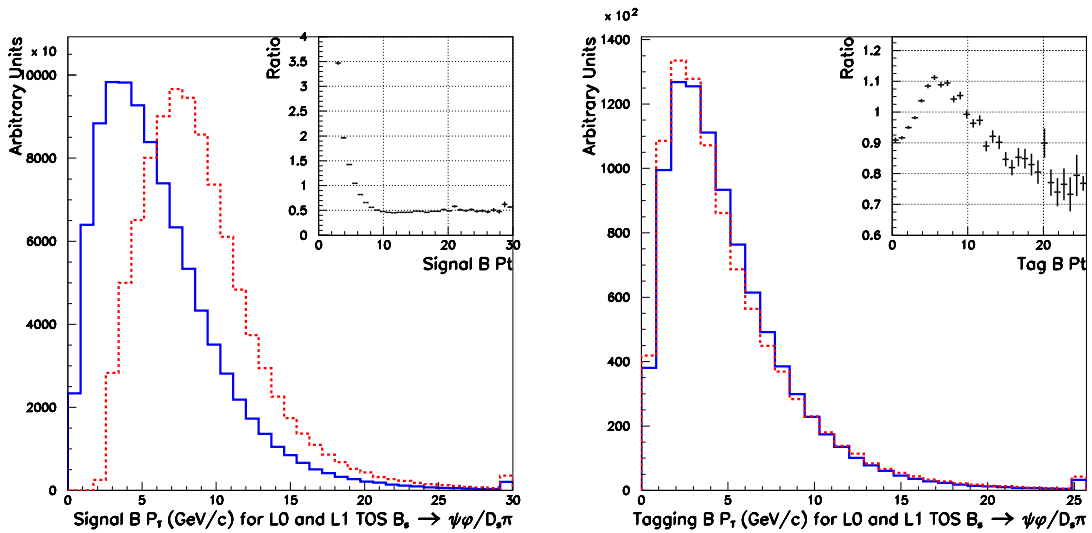


Figure 6 P_T distributions of the signal B in the left and the tagging B in the right for both the control channel (dashed line) and the $B_s \rightarrow J/\psi\phi$ (solid line) after a L0 and L1 TOS trigger selection. The distributions are normalized to have the same area and the ratio of the distributions is shown on the top right corner.

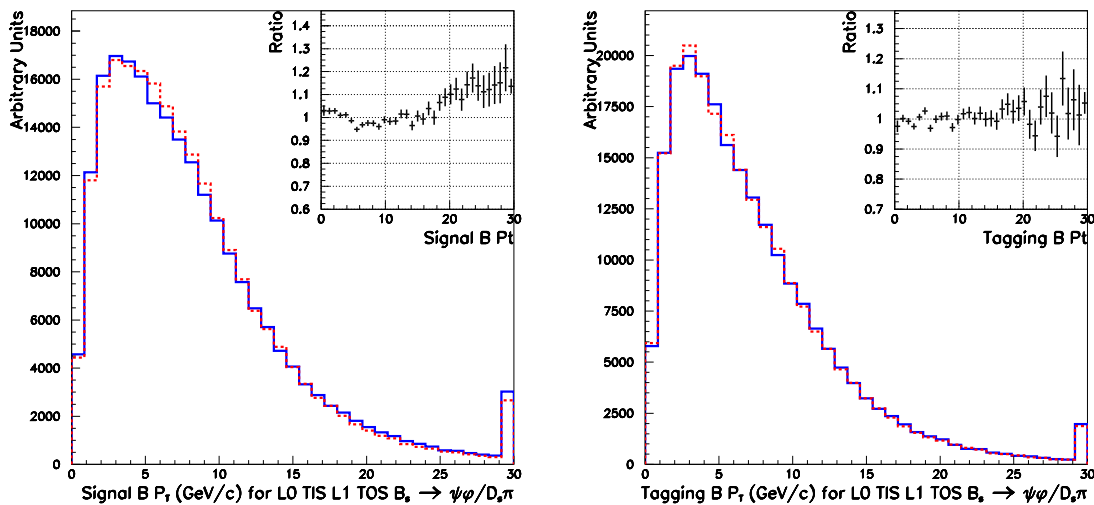


Figure 7 P_T distributions of the signal B in the left and the tagging B in the right for the control channel (dashed line) and the $B_s \rightarrow J/\psi\phi$ (solid line) after a L0 TIS and a L1 TOS selection. The distributions are normalized to have the same area and the ratio of the distributions is shown on the top right corner.

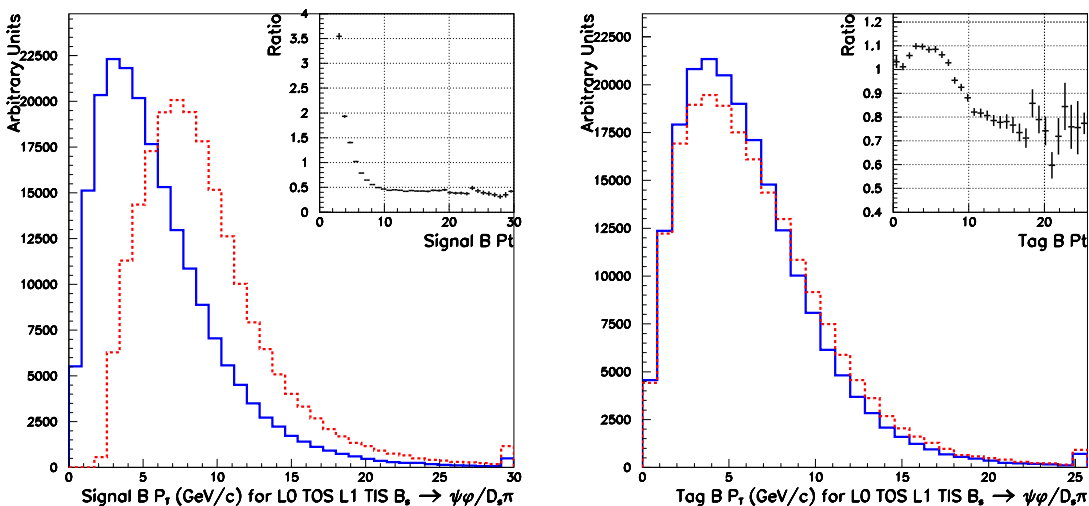


Figure 8 P_T distributions of the signal B in the left and the tagging B in the right for both the control channel (dashed line) and the $B_s \rightarrow J/\psi\phi$ (solid line) after a L0 TOS and a L1 TIS selection. The distributions are normalized to have the same area and the ratio of the distributions is shown on the top right corner.

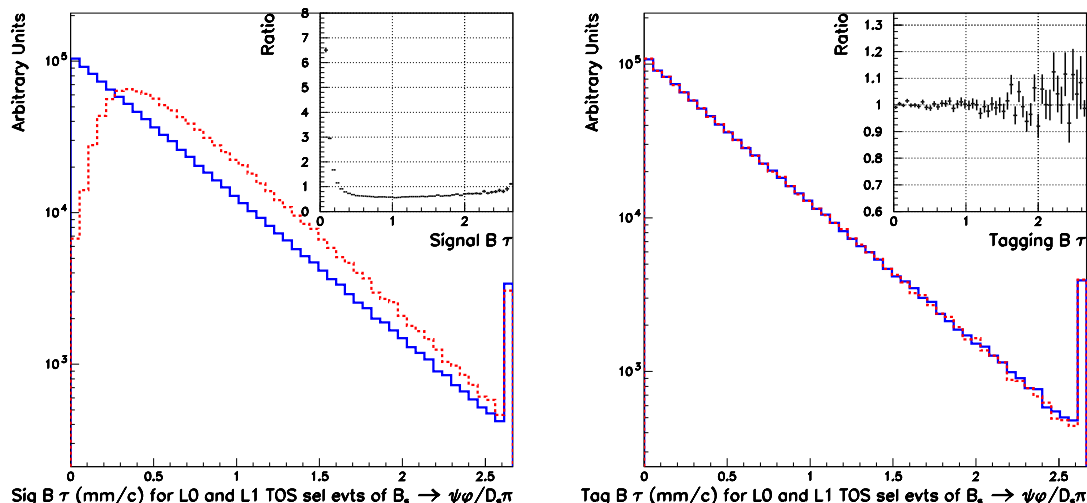


Figure 9 τ distributions of the signal B in the left and the tagging B in the right for both the control channel (dashed line) and the $B_s \rightarrow J/\psi\phi$ (solid line) after a TOS L0 and L1 selection. The distributions are normalized to have the same area and the ratio of the distributions is shown on the top right corner.

reasoning, one expects the L1 TOS samples to have the similar behavior even for the L0 TIS selection. The distributions for this category are presented in figure 10.

Concerning the L1 TIS selection the expectation would be that the bias in the tagging B τ comes from other TOS selections that change the phase space before this selection is applied. So by applying the I_P cuts in these events we end up with τ distributions biased in different ways for each channel. In this sense the two channels L0 TOS samples should have more distinct distributions as the only TOS selection of the whole trigger TIS sample is the geometrical acceptance requirement. Both behaviors can be seen in figures 11 and 12.

So far together with the signal B phase space the tagging B distributions were shown. This was done because the opposite taggers are expected to be mainly products from this hadron. But this is not the case of the same side kaon tagged events. Of course the same reasoning given to explain the tagging B distributions in each trigger category applies to any particle correlated to the signal B. This means that also for the same side kaon phase space we should expect to see clear differences for L0 TOS events and similar distributions for the L0 TIS events. These can be seen in the P_T distributions shown in figures 13 and 14 for events with same side tagging.

4.2 Tagging results

To look for differences in tagging performance due to discrepancies in the phase space the obvious choice of variable is the tagging B transverse momentum because the cuts applied by the tagging algorithm are done also in the P_T of the particles. And in the ideal case the tagging particles originate from this meson. The P_T of the tagging B was shown to be different between channels after trigger selection in the previous section. Therefore the tagging performance should also be expected to be unequal even in the same trigger category. These numbers are shown in tables 9 for the overall tagging and 10 for each of the tagging particles together with the numbers for the $B_s \rightarrow K^+K^-$.

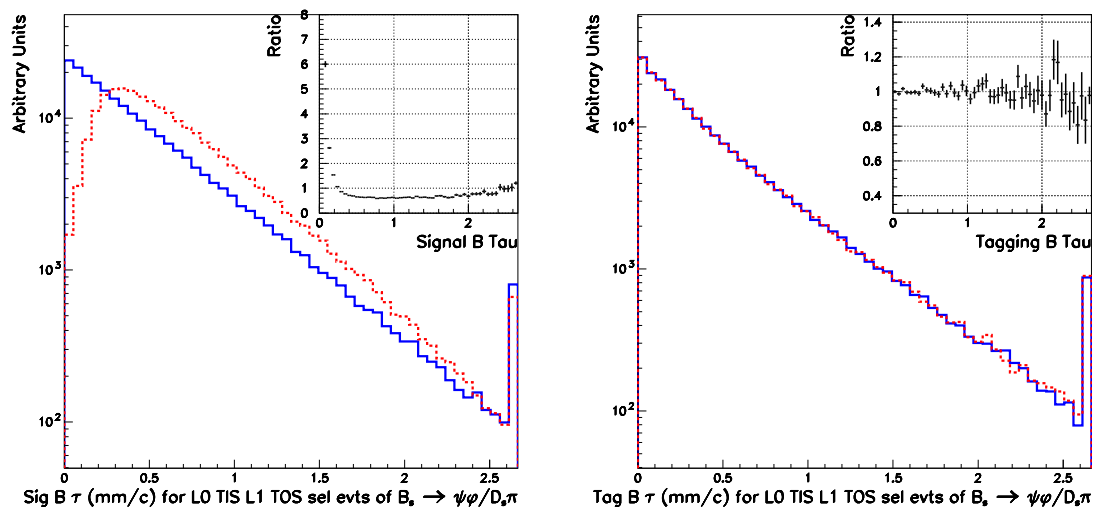


Figure 10 τ distributions of the signal B in the left and the tagging B in the right for both the control channel (dashed line) and the $B_s \rightarrow J/\psi\phi$ (solid line) after a L0 TIS and L1 TOS selection. The distributions are normalized to have the same area and the ratio of the distributions is shown on the top right corner.

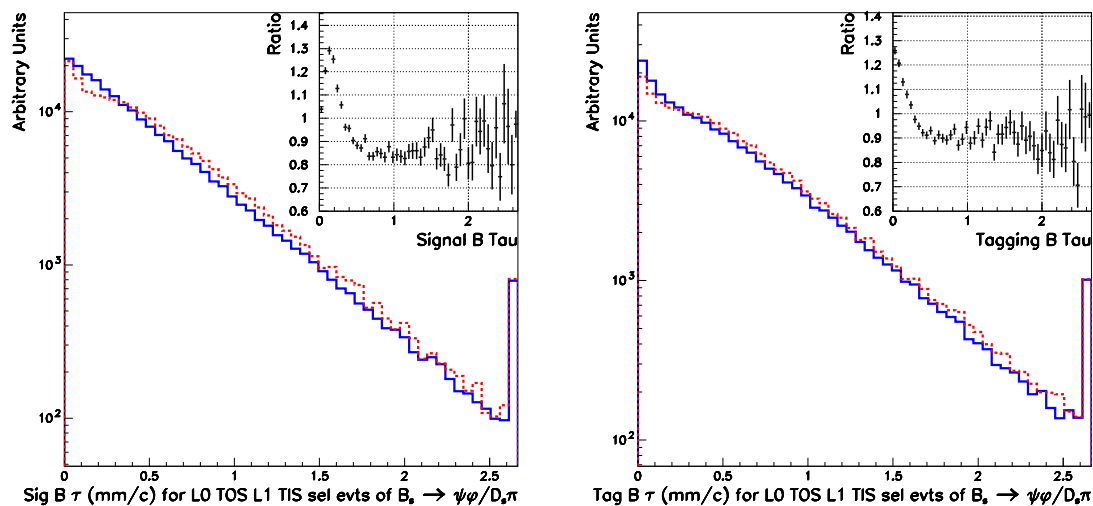


Figure 11 τ distributions of the signal B in the left and the tagging B in the right for both the control channel (dashed line) and the $B_s \rightarrow J/\psi\phi$ (solid line) after a TOS L0 and TIS L1 selection. The distributions are normalized to have the same area and the ratio of the distributions is shown on the top right corner.

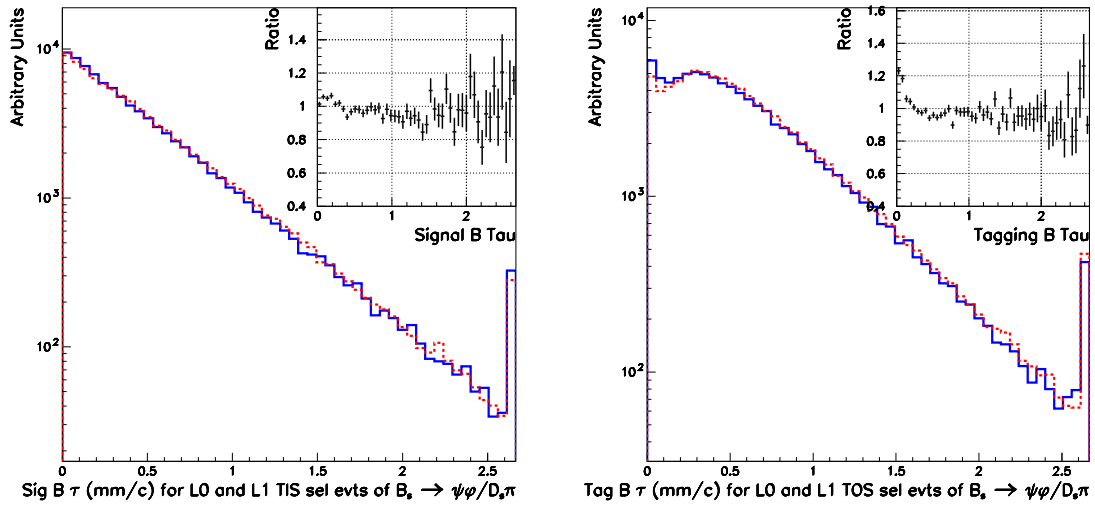


Figure 12 τ distributions of the signal B in the left and the tagging B in the right for both the control channel (dashed line) and the $B_s \rightarrow J/\psi\phi$ (solid line) after a TIS L0 and L1 selection. The distributions are normalized to have the same area and the ratio of the distributions is shown on the top right corner.

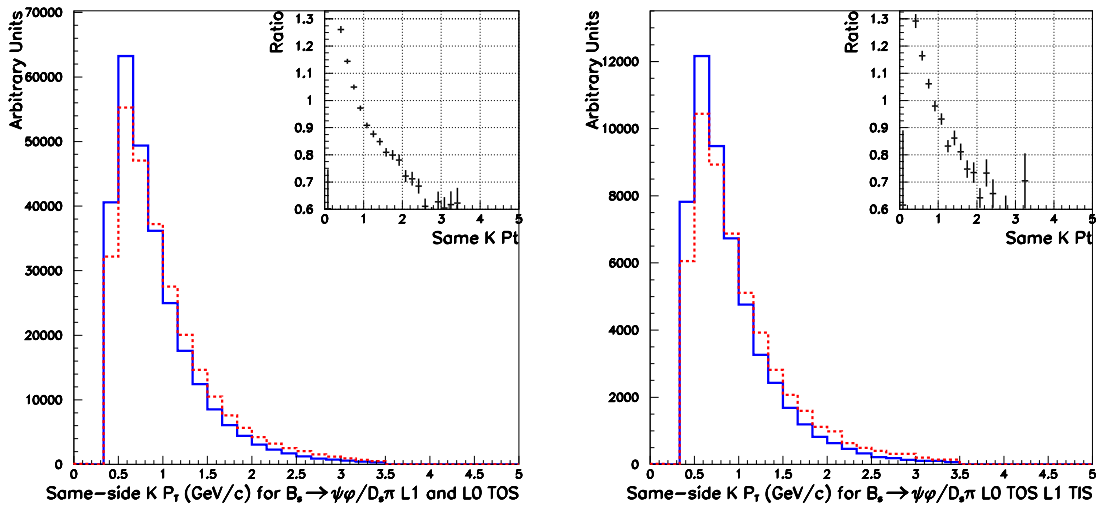


Figure 13 P_T distributions of the same side kaon of L0 TOS selected events for L1 TOS in the left and L1 TIS in the right for both the control channel (dashed line) and the $B_s \rightarrow J/\psi\phi$ (solid line). The distributions are normalized to have the same area and the ratio of the distributions is shown on the top right corner.

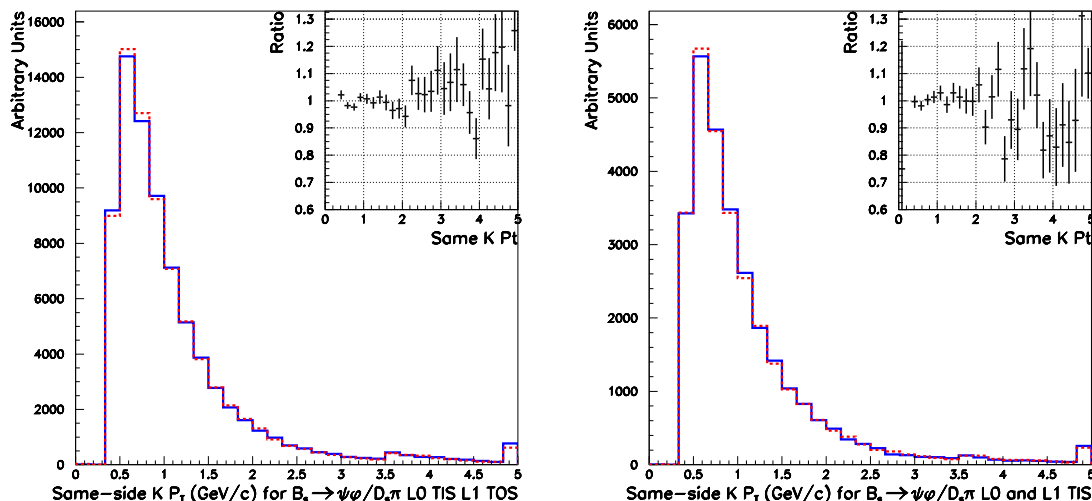


Figure 14 p_T distributions of the same side kaon of L0 TIS selected events for L1 TOS in the left and L1 TIS in the right for both the control channel (dashed line) and the $B_s \rightarrow J/\psi\phi$ (solid line). The distributions are normalized to have the same area and the ratio of the distributions is shown on the top right corner.

channel		L0 TIS			L0 TOS		
		L1 TIS	L1 TOS	L1 TOB	L1 TIS	L1 TOS	L1 TOB
$B_s \rightarrow D_s\pi$	ϵ_{tag}	65.3 ± 0.1	53.5 ± 0.1	58.9 ± 0.2	43.2 ± 0.1	38.49 ± 0.08	41.9 ± 0.2
	ω	22.7 ± 0.2	25.0 ± 0.1	23.6 ± 0.3	22.8 ± 0.2	26.4 ± 0.1	24.2 ± 0.3
	ϵ_{eff}	19.4 ± 0.1	13.40 ± 0.08	16.4 ± 0.2	12.8 ± 0.1	8.54 ± 0.05	11.1 ± 0.1
$B_s \rightarrow J/\psi\phi$	ϵ_{tag}	64.2 ± 0.2	54.1 ± 0.1	-	36.8 ± 0.1	35.68 ± 0.05	-
	ω	23.2 ± 0.2	25.2 ± 0.1	-	25.2 ± 0.2	28.76 ± 0.08	-
	ϵ_{eff}	18.4 ± 0.1	13.32 ± 0.07	-	9.05 ± 0.06	6.44 ± 0.03	-
$B_s \rightarrow K^+K^-$	ϵ_{tag}	65.0 ± 0.1	53.1 ± 0.2	56.1 ± 0.2	40.4 ± 0.1	35.02 ± 0.08	39.7 ± 0.1
	ω	23.0 ± 0.2	25.7 ± 0.2	23.8 ± 0.2	24.0 ± 0.2	29.1 ± 0.1	25.7 ± 0.1
	ϵ_{eff}	19.0 ± 0.1	12.6 ± 0.1	15.4 ± 0.1	10.94 ± 0.07	6.11 ± 0.04	9.37 ± 0.06

Table 9 Tagging efficiency, wrong tagging fraction and effective tagging efficiency for the studied channels for each trigger selection category.

It is worth saying that all the muon tagged events will be L0 TIS. This happens because the cut applied by this level for a muon to be triggered is the same as the one for a muon to be considered as a tagging particle (table 2). So we have only 2 or 3 categories for this type of tagging depending on the channel having or not the TOB category.

From table 9 we can see that the events in L0 TIS categories have similar tagging performance while the L0 TOS selection creates a big difference between signal and control channels. This behavior should be expected as it is the same observed for the phase space differences shown in the previous section. From table 10 another clear effect is that the same side tagging performance is much more affected by the selection than the opposite side taggers. This is due to the kinematic cuts applied to this tag. They are linked to the signal B variables. Being so, this type of tagging is more sensitive to differences between channels. On the other hand the difference in the other taggers comes only through the correlation making their performances more similar.

Tag		μ					
Trigger		$B_s \rightarrow D_s\pi$		$B_s \rightarrow J/\psi\phi$		$B_s \rightarrow K^+K^-$	
L0	L1	ϵ_{tag}	ω	ϵ_{tag}	ω	ϵ_{tag}	ω
TIS	TIS	30.0 ± 0.1	29.0 ± 0.2	29.2 ± 0.2	28.7 ± 0.3	30.4 ± 0.1	29.3 ± 0.2
TIS	TOS	20.1 ± 0.1	23.9 ± 0.2	20.3 ± 0.1	24.1 ± 0.2	22.7 ± 0.1	23.1 ± 0.3
TIS	TOB	24.6 ± 0.2	25.9 ± 0.4	-	-	21.3 ± 0.1	24.7 ± 0.3
Total		9.43 ± 0.03	26.5 ± 0.2	4.81 ± 0.02	25.8 ± 0.2	7.23 ± 0.03	26.5 ± 0.2
Tag		e					
Trigger		$B_s \rightarrow D_s\pi$		$B_s \rightarrow J/\psi\phi$		$B_s \rightarrow K^+K^-$	
L0	L1	ϵ_{tag}	ω	ϵ_{tag}	ω	ϵ_{tag}	ω
TIS	TIS	14.7 ± 0.1	28.9 ± 0.3	14.3 ± 0.1	29.4 ± 0.4	14.9 ± 0.1	28.7 ± 0.3
TIS	TOS	8.97 ± 0.07	22.8 ± 0.3	9.10 ± 0.06	22.6 ± 0.3	9.6 ± 0.1	22.4 ± 0.4
TIS	TOB	10.8 ± 0.2	25.3 ± 0.7	-	-	9.5 ± 0.1	25.0 ± 0.5
TOS	TIS	6.02 ± 0.07	30.9 ± 0.6	5.05 ± 0.05	29.8 ± 0.4	5.87 ± 0.06	30.0 ± 0.5
TOS	TOS	2.97 ± 0.03	26.5 ± 0.4	3.08 ± 0.02	26.3 ± 0.3	2.93 ± 0.03	25.7 ± 0.4
TOS	TOB	4.67 ± 0.08	26.4 ± 0.8	-	-	3.87 ± 0.04	26.1 ± 0.5
Total		6.74 ± 0.03	26.7 ± 0.2	4.94 ± 0.02	26.3 ± 0.2	6.14 ± 0.02	26.7 ± 0.2
Tag		K_{opp}					
Trigger		$B_s \rightarrow D_s\pi$		$B_s \rightarrow J/\psi\phi$		$B_s \rightarrow K^+K^-$	
L0	L1	ϵ_{tag}	ω	ϵ_{tag}	ω	ϵ_{tag}	ω
TIS	TIS	28.1 ± 0.1	18.0 ± 0.2	26.3 ± 0.3	18.2 ± 0.3	28.1 ± 0.1	18.4 ± 0.2
TIS	TOS	8.51 ± 0.07	19.0 ± 0.3	8.78 ± 0.06	19.3 ± 0.3	8.73 ± 0.09	18.8 ± 0.4
TIS	TOB	12.6 ± 0.2	19.0 ± 0.6	-	-	11.2 ± 0.1	18.8 ± 0.4
TOS	TIS	18.3 ± 0.1	19.8 ± 0.3	14.39 ± 0.08	19.5 ± 0.2	17.73 ± 0.09	19.7 ± 0.2
TOS	TOS	7.98 ± 0.05	20.6 ± 0.2	8.23 ± 0.03	20.4 ± 0.1	8.06 ± 0.05	20.9 ± 0.2
TOS	TOB	12.2 ± 0.1	20.1 ± 0.4	-	-	10.94 ± 0.06	20.2 ± 0.3
Total		12.83 ± 0.04	19.3 ± 0.1	10.26 ± 0.03	19.7 ± 0.1	12.94 ± 0.03	19.6 ± 0.1
Tag		K_{same}					
Trigger		$B_s \rightarrow D_s\pi$		$B_s \rightarrow J/\psi\phi$		$B_s \rightarrow K^+K^-$	
L0	L1	ϵ_{tag}	ω	ϵ_{tag}	ω	ϵ_{tag}	ω
TIS	TIS	32.1 ± 0.1	30.2 ± 0.2	32.0 ± 0.2	30.6 ± 0.3	30.4 ± 0.1	30.3 ± 0.2
TIS	TOS	34.2 ± 0.1	31.8 ± 0.2	34.6 ± 0.1	32.1 ± 0.2	30.1 ± 0.1	35.2 ± 0.3
TIS	TOB	35.5 ± 0.2	29.4 ± 0.4	-	-	35.2 ± 0.2	29.5 ± 0.3
TOS	TIS	30.5 ± 0.1	26.0 ± 0.2	25.5 ± 0.1	29.7 ± 0.2	27.2 ± 0.1	28.3 ± 0.2
TOS	TOS	32.34 ± 0.08	28.6 ± 0.1	28.85 ± 0.05	31.94 ± 0.09	28.32 ± 0.08	32.3 ± 0.2
TOS	TOB	32.7 ± 0.2	27.0 ± 0.3	-	-	31.3 ± 0.1	28.6 ± 0.2
Total		32.63 ± 0.05	29.09 ± 0.09	29.43 ± 0.04	31.61 ± 0.07	29.73 ± 0.04	30.58 ± 0.08

Table 10 Tagging efficiency and ω for the studied channels in the trigger selection categories for each tagging particle used in the simulation.

4.3 Wrong tagging fraction correction

It was argued previously in section 3.1 that ω is expected to be the same for any channel if one looks only inside an infinitesimal small volume of the signal B phase space, for each trigger category. Being so, for every signal event one should use only the control channel events with the same phase space to measure its ω . The size of the volume in phase space around a signal channel event in which one looks for a tagging answer has to be a compromise between the precision wanted in ω and the statistics we want to throw away. This happens because if it is tried to look in a too small phase space region around a given signal channel event it is very likely that there is no correspondence in the control channel. And when this is the case the event has to be discarded. On the other hand if one takes a too big volume for the correction there will be events that are not representative for the signal being used to extract ω . And the later case will of course bring a systematic error in the measurement of ω .

Some assumptions are made to simplify the problem. Having in mind that both trigger and tagging cuts are done mainly on the P_T this is the only variable considered for the correction. So for every $J/\psi\phi$ event one has to take all control channel events around a certain slice of the signal channel P_T to get a ω answer. What happens by doing so is that instead of having an answer from the tagging that is either right or wrong for a given signal event (as is the case for the control channels) we have a fractional value per signal event, which gives the probability of having the wrong tagging answer assigned to it from the $D_s\pi$ sample.

It is also assumed that the error in this ω assigned to each $J/\psi\phi$ event is the binomial error of the ratio of wrongly tagged and the number of tagged events used from the control sample to get to this ω value. In practice instead of taking every $J/\psi\phi$ event they are grouped into sufficiently small P_T -bins.

An important feature of the problem can be noticed from all the transverse momentum plots shown before. It is clear that there are much more events with lower signal $B_s P_T$ than with higher values. So it is not sensible to use the same size of P_T slice in the whole range. It would be a waste of bins in the higher region where there are fewer events so the precision doesn't need to be as good as in the small and highly populated part of the P_T spectra.

To deal with these features of the problem the correction was done using different sizes of P_T slices in each trigger category. Following the argument given above the way to go was to put the same amount of events in each phase space slice. As the $B_s \rightarrow J/\psi\phi$ populates some parts of the spectrum in this variable that the control channel doesn't, the choice was made to separate the bins by equally populating them with signal channel events. By doing so we end up with variable bin sizes shown in figures 15 and 16.

In practice the arguments given above mean that we can expect that the wrong tagging fraction distributions of the samples, as a function of P_T , should overlap within each trigger category. Using the unequal sized binning explained previously this can be verified for all categories in figures 17 and 18.

Another important characteristic of this method for these specific channels can be seen by comparing the signal B distributions for the L0 TOS selected events of figures 6 and 8. By doing so it is clear that there are small P_T signal events in the $J/\psi\phi$ samples that do not appear in the control channel sample. This means that we cannot look for a correction for these events in this signal $D_s\pi$ phase space and hence they have to be discarded.

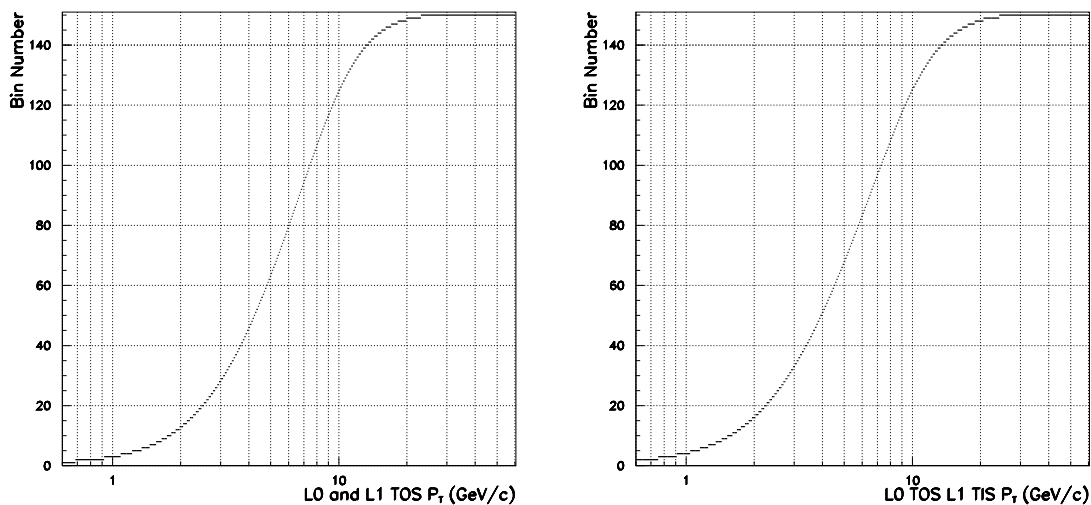


Figure 15 Bin number as a function of P_T for 150 equally populated bins with $B_s \rightarrow J/\psi\phi$ events for L0 TOS. L1 TOS is shown in the left plot and L1 TIS in the right. The size of the bins are given by the length of the points in the x axis.

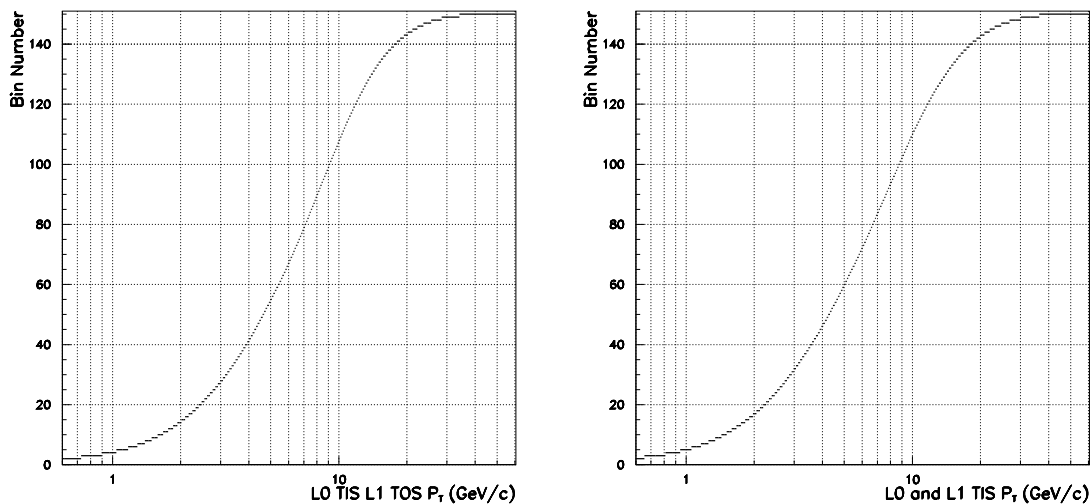


Figure 16 Bin number as a function of P_T for 150 equally populated bins with $B_s \rightarrow J/\psi\phi$ events for L0 TIS. L1 TOS is shown in the left plot and L1 TIS in the right. The size of the bins are given by the length of the points in the x axis.

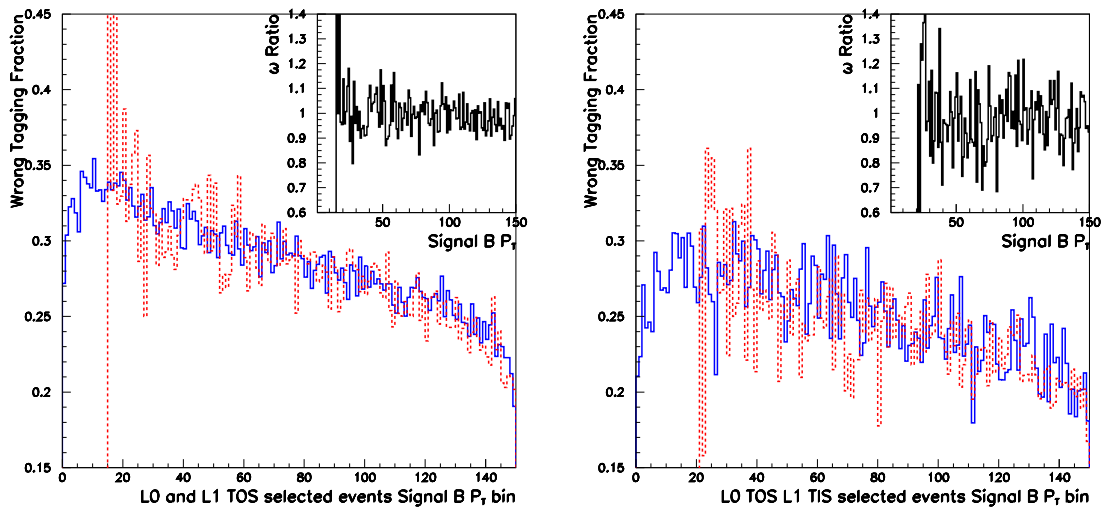


Figure 17 Wrong tagging fraction as a function of the transverse momentum bins of figure 15 for L0 TOS selected events. L1 TOS is shown in the left and L1 TIS in the right. The $B_s \rightarrow J/\psi\phi$ is the solid and the control the dashed lines. The ω ratios are shown in the top right corner in each case. The error bars were hidden for the clarity of the plots.

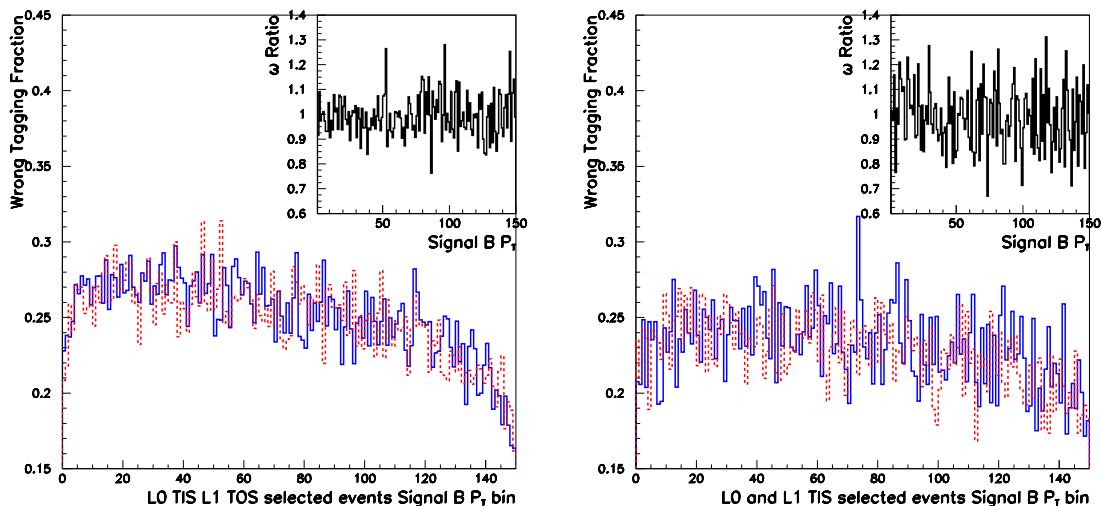


Figure 18 Wrong tagging fraction as a function of transverse momentum bins of figure 16 for L0 TIS selected events. L1 TOS is shown in the left and L1 TIS in the right. The $J/\psi\phi$ is the solid and the control the dashed line. The ω ratios are shown in the top right corner in each case. The error bars were hidden for the clarity of the plots.

	L0 TIS		L0 TOS	
	L1 TIS	L1 TOS	L1 TIS	L1 TOS
% Discarded	-	-	10.4	13.7
New ω	22.7 ± 0.2	25.0 ± 0.1	24.7 ± 0.2	28.23 ± 0.08

Table 11 Amount of discarded events for not having a correspondence in the control channel phase space and the wrong tagging fraction obtained with the remaining events. Only the L0 TOS events are affected. This translates into a total loss of 8.8%

The number of discarded events is shown for each category in table 11 together with the new ω values obtained without these events. In this particular case it meant discarding 8.8% of the events.¹

Then for every $J/\psi\phi$ event in each of the trigger categories we look for an ω answer in the $D_s\pi$ sample only in events that fall into a certain P_T -interval around this event signal $B_s P_T$ value. The ω values obtained as a function of the P_T -interval size are shown in figures 19 and 20 for each of the trigger categories present in the $J/\psi\phi$. In these, the x-axis represents the number of bins around the signal $B P_T$ that were looked at in the control channel sample to assign the ω value for each event. At the smallest P_T interval every signal channel event was considered to have the ω obtained only with the events that fell into the same P_T bin of the $D_s\pi$ distributions 17 and 18. The second is where for every $J/\psi\phi$ event one takes also the $D_s\pi$ events that fall into one P_T bin to the left and one to the right of the same distributions to assign the ω for each event and so on. And the last point means we do no correction and assign the overall $D_s\pi$ ω value to every signal channel event.

In the same way as the ω itself the error is assigned per event. It was explained how, for a given P_T interval, the ω is obtained using a certain number of control channel events. The error is then given by the binomial error of these $B_s \rightarrow D_s\pi$ events. Therefore, for smaller P_T intervals the per event error in ω is bigger as less events were used to obtain the wrong tagging fraction value. Since the number of signal channel events is always the same, the overall ω error is also bigger in this region.

Another feature of this procedure is that the whole control sample is used in all intervals. But for the smallest interval each control channel event is used only for the signal channel events that fell into the same P_T bin as itself. By making the intervals bigger they are also used for other events. Until arriving to the biggest interval where every $B_s \rightarrow D_s\pi$ event is used to obtain ω for all the $B_s \rightarrow J/\psi\phi$ sample. This implies that there is a big correlation both in ω and in the error values between different P_T intervals. This can be understood thinking of a single signal channel event. When going to a bigger interval one is making the interval around the P_T value wider and therefore, adding a few events to the same events used in the previous interval to obtain ω .

Also in figures 19 and 20 are shown the ω values obtained with MC-truth information from the $B_s \rightarrow J/\psi\phi$ sample. From these plots it is noticeable that for the L0 TIS categories the correction makes little (if any) difference as could be expected as both the P_T spectra and the ω values were similar between channels before the correction. On the other hand in the L0 TOS categories there was originally disagreement in ω . Looking at the plots we can see that narrowing the P_T -interval reduces the discrepancy between

¹On top of that for this study it was chosen to pick up an extreme case of difference in bias in very different kinematic channels to prove the method to be valid. Hence it can be expected that in the real data the amount of rejected events to be smaller with the choice of control channels which are more similar to the signal kinematics and trigger bias. For instance the $B_d \rightarrow J/\psi K^*$ is a good candidate of having the same phase space as $B_s \rightarrow \phi\phi$, and could be used to obtain ω for opposite-side tags.

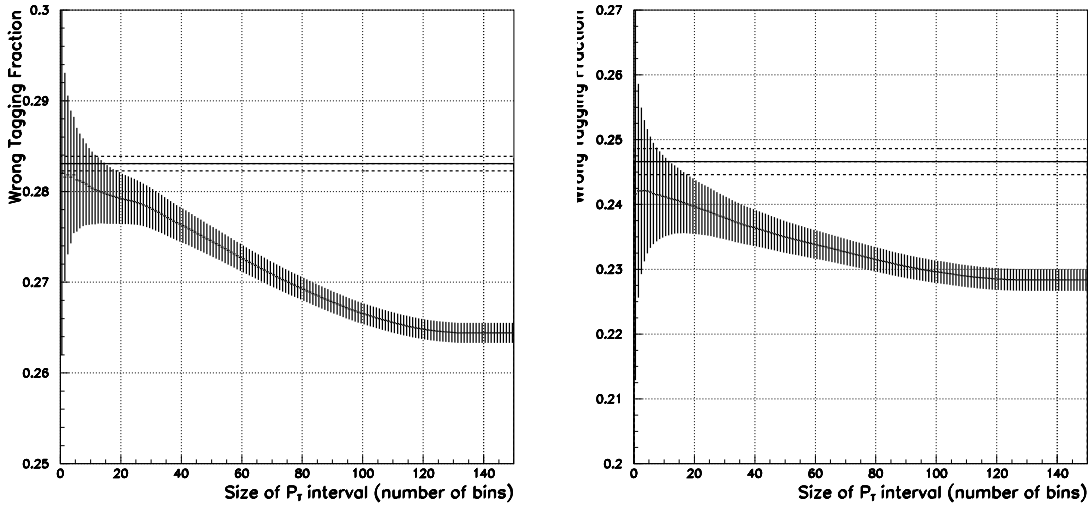


Figure 19 The points with error bars represent the wrong tagging fraction obtained from the $B_s \rightarrow D_s\pi$ for each P_T interval used. The solid line is the actual ω of the signal channel sample considering only the events that were not discarded and the dashed line replaces the error bars for this signal channel. The x-axis represents each P_T interval used, expressed in number of bins in the $\omega(P_T)$ distributions used to obtain the ω for each $J/\psi\phi$ event (figure 17). The L1 TOS category is shown in the left and the L1 TIS in the right for L0 TOS selected events.

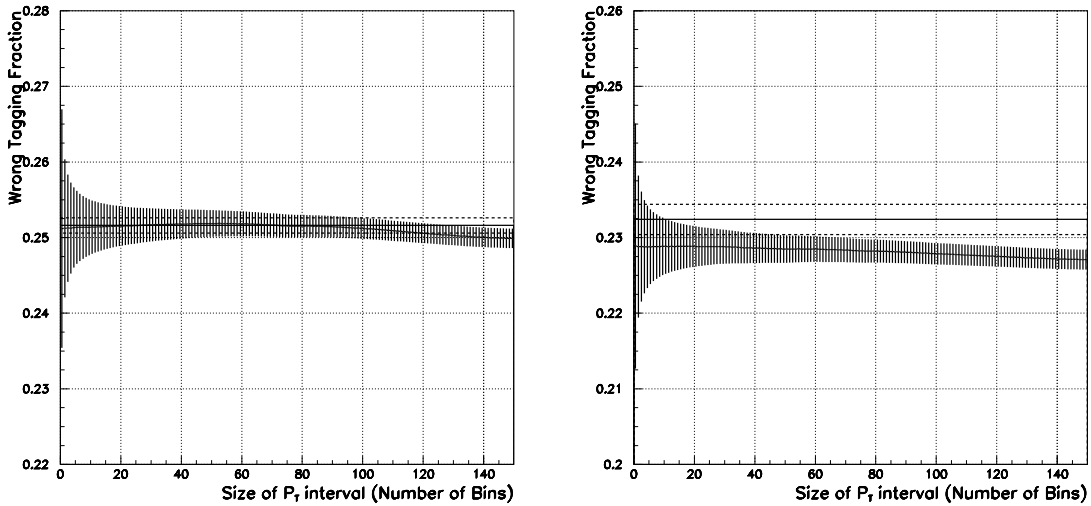


Figure 20 The points with error bars represent the wrong tagging fraction obtained from the $B_s \rightarrow D_s\pi$ for each P_T interval used. The solid line is the actual ω of the signal channel sample. The dashed line replaces the error bars for the signal channel value. The x-axis represents each P_T interval expressed in the number of bins in the $\omega(P_T)$ distributions used to obtain the ω for every $J/\psi\phi$ event (figure 18). The L1 TOS category is shown in the left and the L1 TIS in the right for L0 TIS selected events.

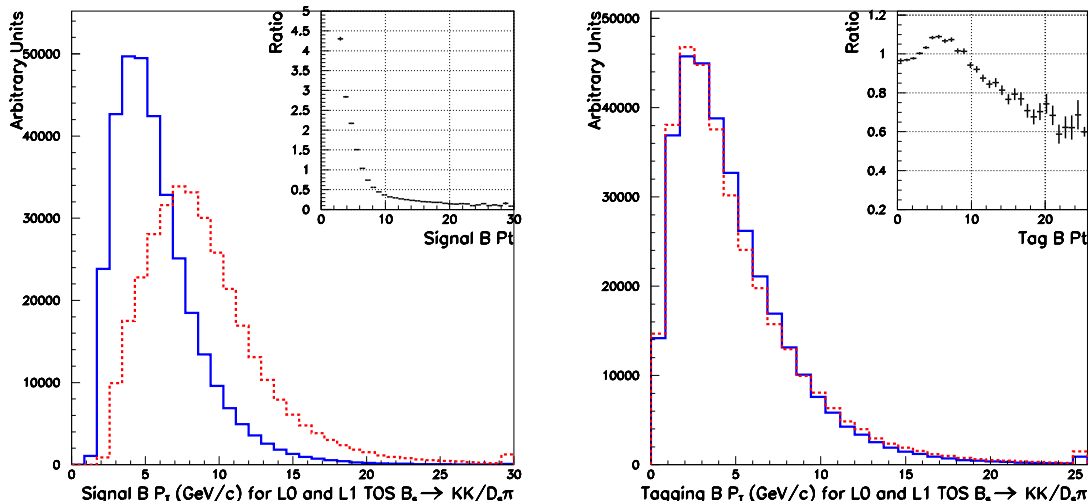


Figure 21 P_T distributions of the signal B in the left and the tagging B in the right for both the control channel (dashed line) and the $B_s \rightarrow K^+K^-$ (solid line) after a L0 and L1 TOS trigger selection. The distributions are normalized to have the same area and the ratio of the distributions is shown on the top right corner.

the values of ω obtained from the control and the MC signal samples. Eventually the ω obtained from the control sample gets into a small plateau that is compatible with the true value.

The correction method is enough to extract a correct wrong tagging fraction value for the $B_s \rightarrow J/\psi\phi$ using as control channel the $B_s \rightarrow D_s\pi$. Considering the large disagreement before any correction was done and the considerable difference in bias due to the di-muon trigger it is a very good test for the method. This exaggerated difference in the bias caused that a number of events had to be discarded.

5 $B_s \rightarrow K^+K^-$

It was shown that the method works properly to extract ω for the $B_s \rightarrow J/\psi\phi$. But this channel has the convenience of not having any TOB events. It is not the case for every signal channel and looking at table 8 we see that this kind of events represents a big proportion of the $B_s \rightarrow K^+K^-$. This happens because the L1 is a two particle trigger and then it is more likely in a channel with only two tracks in the final state that the event is triggered by one of these particles together with some track from elsewhere.

The same procedure followed in the correction of the $B_s \rightarrow J/\psi\phi$ is used for this signal channel. The first noticeable difference appears by comparing the signal B P_T distributions of L0 TOS selected events of the control channel and the $B_s \rightarrow K^+K^-$ in figures 21 and 22. In these one can verify that the phase space occupied by both channels is very similar (considering only the transverse momentum as phase space variable). Being so in this case only a very small quantity of signal events have to be discarded in these categories. These numbers are shown in table 12 together with the new values for ω , obtained without these events.

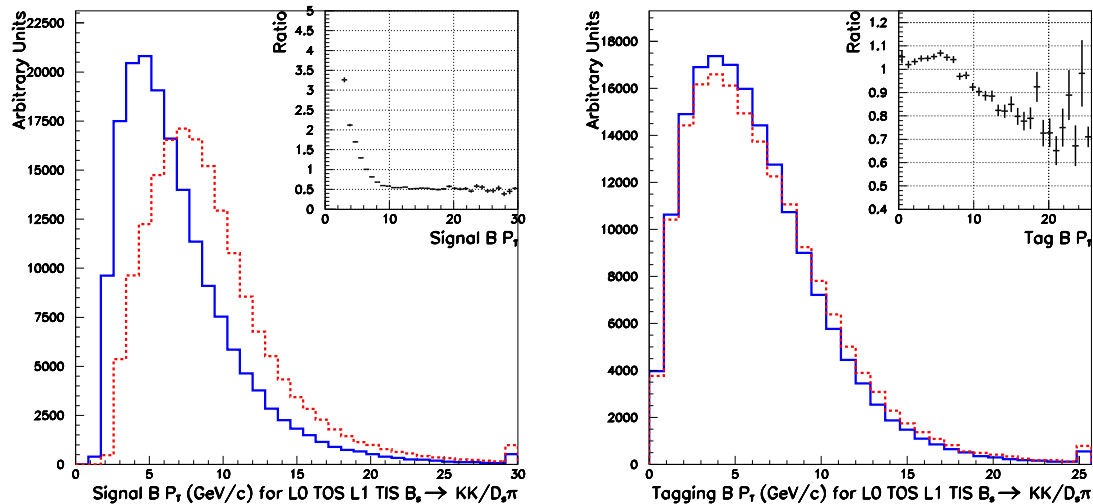


Figure 22 P_T distributions of the signal B in the left and the tagging B in the right for both the control channel (dashed line) and the $B_s \rightarrow K^+K^-$ (solid line) after a L0 TOS and L1 TIS trigger selection. The distributions are normalized to have the same area and the ratio of the distributions is shown on the top right corner.

	L0 TIS			L0 TOS		
	L1 TIS	L1 TOS	L1 TOB	L1 TIS	L1 TOS	L1 TOB
% Discarded	-	-	-	3.8	2.7	1.9
New ω	23.0 ± 0.2	25.7 ± 0.2	23.8 ± 0.2	23.9 ± 0.2	29.0 ± 0.1	25.6 ± 0.1

Table 12 Amount of discarded events for not having a correspondence in the control channel phase space and the wrong tagging fraction obtained with the remaining events. Only the L0 TOS events are affected. This numbers translate into discarding 1.7% of the events.

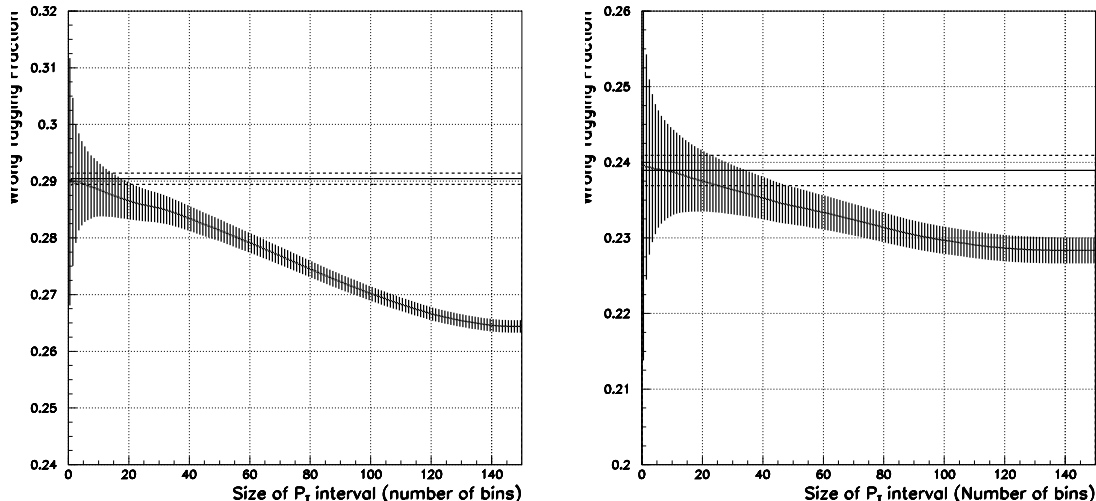


Figure 23 The points with error bars represent the wrong tagging fraction obtained from the $B_s \rightarrow D_s\pi$ for each P_T interval used. The solid line is the actual ω of the signal channel sample considering only the events that were not discarded and the dashed line replaces the error bars for this signal channel. The x-axis represents each P_T interval used, expressed in number of bins in the $\omega(P_T)$ distributions used to obtain the ω for each K^+K^- event. The L1 TOS category is shown in the left and the L1 TIS in the right for L0 TOS selected events.

The ω correction method applied to this channel is shown in figures 23 and 24. For the correction the binning was chosen by equally populating the spectra with $B_s \rightarrow K^+K^-$ events. Table 9 attests that, unlike the $J/\psi\phi$ case, in the L0 TIS, L1 TOS category ω did not have a compatible value before the correction.

The plots show that the correction works very well in all trigger categories where there was a disagreement in ω . The plateau reached at the small P_T -intervals attests that applying the correction method would give us the right value for the wrong tagging fraction of the $B_s \rightarrow K^+K^-$ looking only in the control channel.

5.1 TOB events

Nevertheless, the biggest difference between $B_s \rightarrow J/\psi\phi$ and $B_s \rightarrow KK$ is the presence of TOB events. It was argued in section 3 that categories with TOB events have more complicated systematics to treat than the TIS and TOS ones. For lack of a better method we apply the same method used previously and check the results. The P_T distributions of the b hadrons are shown in figures 25 and 26 for the two L1 TOB categories.

One can notice the same behaviour as for the $B_s \rightarrow J/\psi\phi$, where the L0 TOS selection is responsible for the major differences in the P_T distributions. This can also be seen in the numbers for ω from table 9. Following the correction method ω is obtained from the control channel and the results of the correction are shown in figure 27. The amount of discarded events for L0 TOS is shown, together with the value of ω obtained without these events, in table 12.

From the results of the correction we see that, even if a plateau is reached for L0 TOS, when it happens it does not overlap with the actual MC ω value of the signal channel as happened in the other categories. This only happens in the smallest P_T intervals but

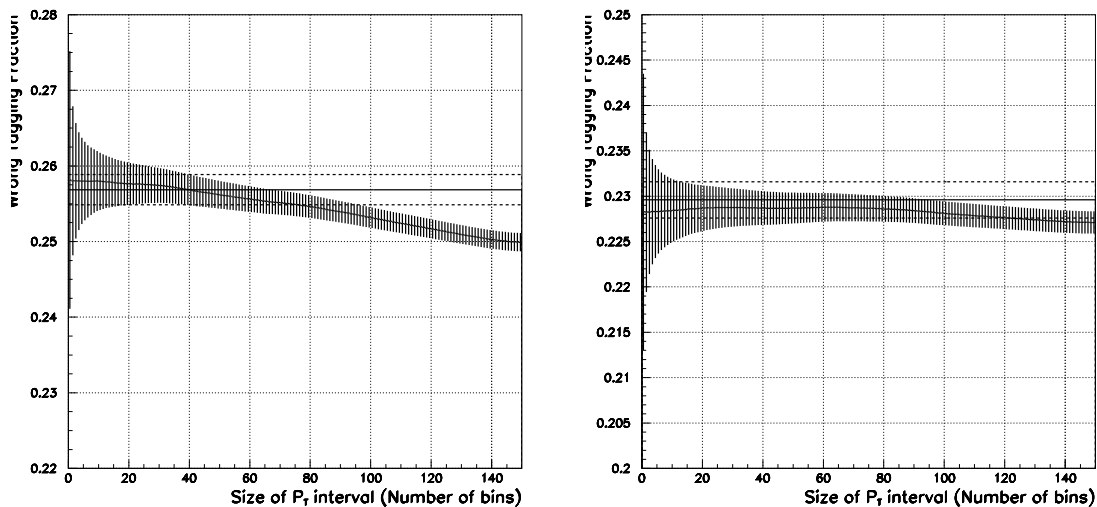


Figure 24 The points with error bars represent the wrong tagging fraction obtained from the $B_s \rightarrow D_s\pi$ for each P_T interval used. The solid line is the actual ω of the signal channel and the dashed line replaces the error bars for this signal channel value. The x-axis represents each P_T interval used, expressed in number of bins in the $\omega(P_T)$ distributions used to obtain the ω for each K^+K^- event. The L1 TOS category is shown in the left and the L1 TIS in the right for L0 TIS selected events.

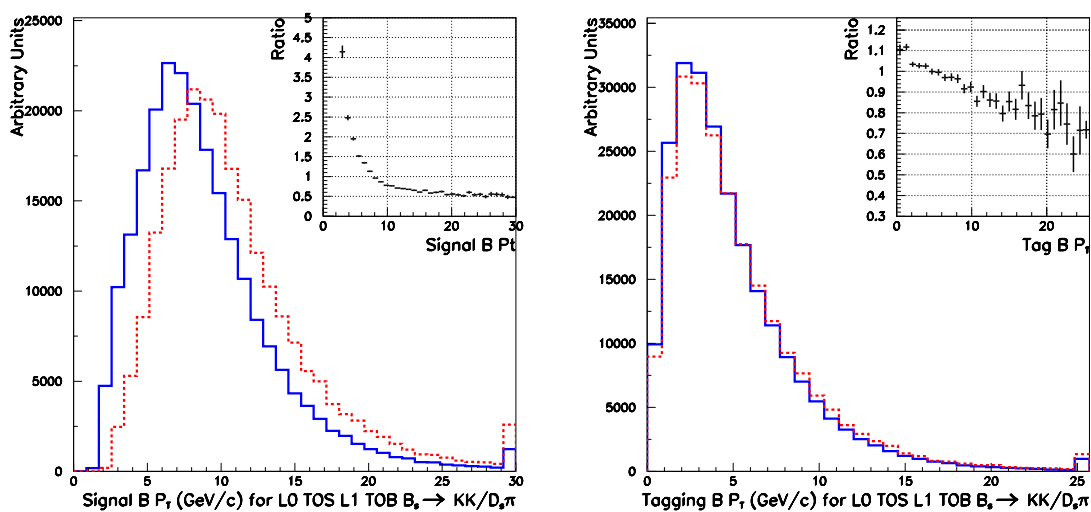


Figure 25 P_T distributions of the signal B in the left and the tagging B in the right for both the control channel (dashed line) and the $B_s \rightarrow K^+K^-$ (solid line) after a L0 TOS and L1 TOB trigger selection. The distributions are normalized to have the same area and the ratio of the distributions is shown on the top right corner.

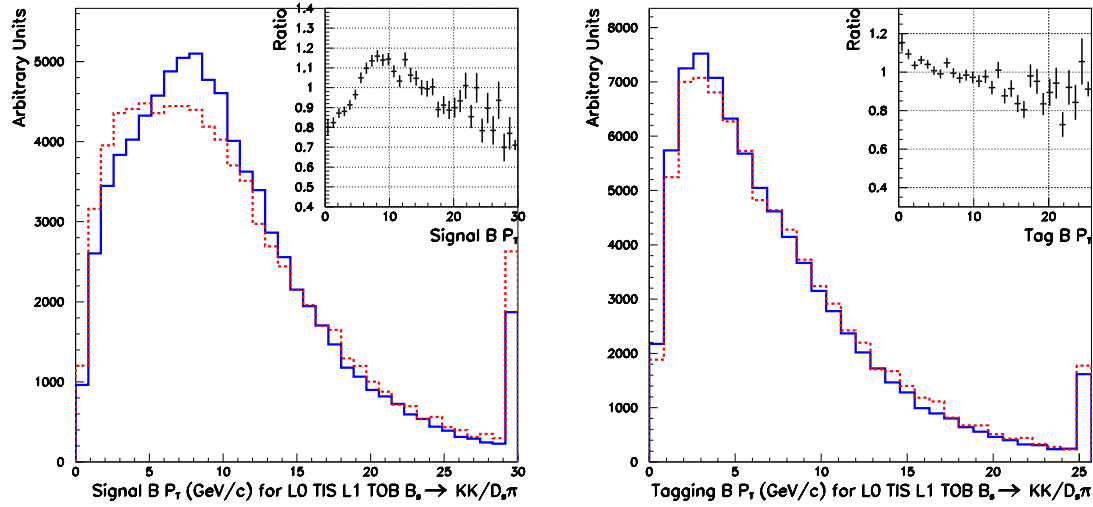


Figure 26 P_T distributions of the signal B in the left and the tagging B in the right for both the control channel (dashed line) and the $B_s \rightarrow K^+K^-$ (solid line) after a L0 TIS and L1 TOB trigger selection. The distributions are normalized to have the same area and the ratio of the distributions is shown on the top right corner.

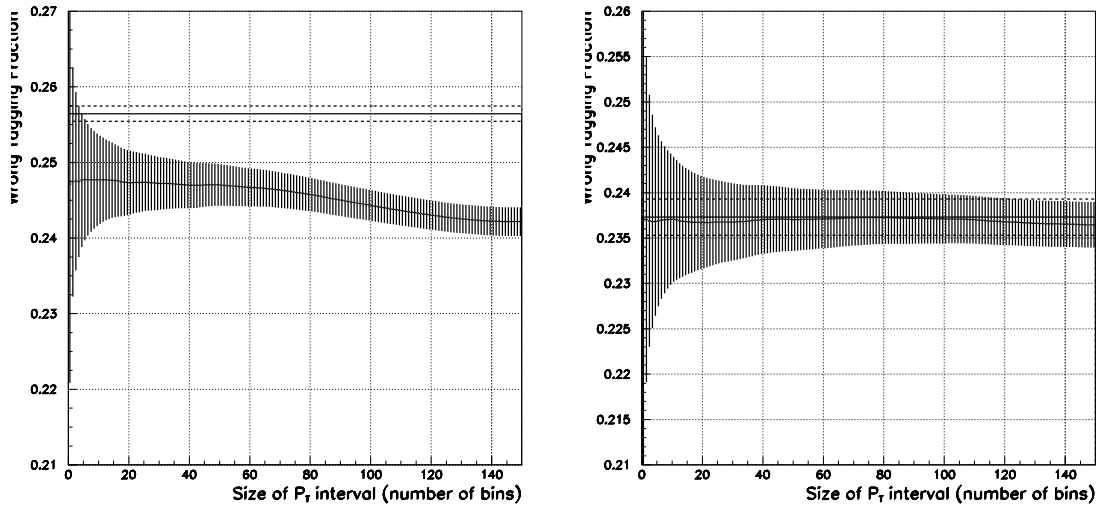


Figure 27 The points with error bars represent the wrong tagging fraction obtained from the $B_s \rightarrow D_s\pi$ for each P_T interval used. The solid line is the actual ω of the signal channel sample considering only the events that were not discarded and the dashed line replaces the error bars for this signal channel. The x-axis represents each P_T interval used, expressed in number of bins in the $\omega(P_T)$ distributions used to obtain the ω for each K^+K^- event. The L0 TOS category is shown in the left and the L0 TIS in the right for L1 TOB selected events.

just because the errors in ω get higher. For L0 TIS the values were compatible to start with so, as expected, the correction does very little to ω value.

With these results if one wants a correct value of ω the TOB events have to be discarded. In the case of two particles in the final state this would represent a major lost of statistics. In this particular case it corresponds to 30% of the events. This difficulty to treat the systematics of these events led to a new design of the trigger to avoid them by creating a single particle trigger also at L1 [6]. $B \rightarrow hh$ channels are predominantly triggered by this single hadron trigger, and hence cannot be classified as as TOB anymore.

6 Conclusion

The effect of the trigger selection was shown to cause a systematic bias in the tagging performance making that the wrong tagging fraction obtained from control channels was different from the one in signal channels. This would introduce a serious systematic uncertainty for the measurements LHCb will make. The correction method used to solve that has the big advantage of depending only on the data that will be available (the signal B_s phase space). The correlation between the signal B and the rest of the event that caused the bias is also treated properly by sorting the events in trigger categories.

The method to obtain the right ω of the signal channels from the control sample works fine for TIS and TOS selected events. In this generator level study, where some simplifications were made, the kinematic bias between the channels was exaggerated to test the method and this caused a significant loss of $B_s \rightarrow J/\psi\phi$ events. In the real case this should be diminished.

In the TOB events the systematics are more complicated to treat. The result of this study was one of the reasons that led the trigger system to be redesigned to avoid this type of events.

7 Acknowledgments

I would like to thank Hans Dijkstra for all the ideas and comments both during the development of the work and the writing of this note. I also would like to thank Olav Ullaland for receiving me in the LBD group and for the effort of giving me a complement to my scholarship during the time I spent at CERN. This study was partially supported by CAPES, CNPq and FAPERJ.

8 References

- [1] The LHCb Collaboration, *LHCb Reoptimized Detector Design and Performance Technical Design Report*, CERN-LHCC 2003-30.
- [2] M. Calvi, O. Dormond and M. Musy, *LHCb Flavour Tagging Performance*, LHCb 2003-115

- [3] T. Sjöstrand, *PYTHIA 5.7 and JETSET 7.4 Physics and Manual*, Computer Physics Commun. **82** (1994) 74.
- [4] The LHCb Collaboration, *LHCb Trigger Technical Design Report*, CERN-LHCC 2003-31.
- [5] T. Schietinger, *Level-1: status*, Trigger Meeting 12 May 2003.
- [6] N. Zwahlen, *T-Rec Meeting 10 Oct 2005*<http://agenda.cern.ch/age?a056037>
- [7] <https://uimon.cern.ch/twiki/bin/view/LHCb/LHCbTrigger>
- [8] H. Dijkstra, N. Tuning and N. Brook, *Some Remarks on Systematic Effects of the Trigger and Event Generator Studies*, LHCb 2003-157 TRIG.
- [9] A. D. Peris et al, *LCG-2 User Guide*, Manual Series CERN-LCG-GDEIS-454439